Investigational
Medicinal Chemistry & Pharmacology

Research Article Open Access

Inhibitors of *Plasmodium falciparum* dihydrofolate reductase-thymidylate synthase: In-silico evaluation of phenylpiperazinyl derivatives

Oluwafemi S. Aina[1,2]*, Mujeeb O. Rofiu[1], Kafayat A. Owoseni-Fagbenro[1], Luqman A. Adams[1], Oluwole B. Familoni[1]

Abstract

Background: Resistance to existing antifolate drugs targeting the dihydrofolate reductase (DHFR) enzyme in Plasmodium falciparum is a major obstacle to malaria control. Furthermore, some current drugs have associated toxicity concerns. To address this, we explored new antifolate inhibitors to develop safer and more potent antimalarial drugs.

Methods: We computationally screened hypothetical compounds A1, A2, and A3 (a parent compound and two alcohol derivatives) for their toxicity and inhibitory effectiveness against the bifunctional DHFR-thymidylate synthase enzyme. Their physicochemical properties, drug-likeness, toxicity, and binding energies were compared to ten standard antimalarial drugs using computational tools like Molinspiration, SwissADME, Protox II, and AutoDock Vina. Density functional theory (DFT) studies were also conducted to understand the electronic properties influencing binding.

Results: All three compounds (A1, A2, and A3) were predicted to be non-toxic and showed favorable drug-like properties, including high gastrointestinal absorption. Compound A1 exhibited a strong binding score of -9.20 kcal/mol, comparable to the drug Artesunate. A2 and A3 also showed potent binding scores of -8.8 kcal/mol and -8.2 kcal/mol, respectively, surpassing Mefloquine. DFT studies revealed a correlation between the binding trend and the compounds' electron affinity (EA) and electronic chemical potential (μ) values.

Conclusion: The results suggest that our investigated compounds, particularly A1 and A3, are promising, non-toxic candidates for further development as antimalarial drugs.

Keywords: *Plasmodium falciparum*; dihydrofolate reductase; molecular docking; piperazine derivatives.

*Correspondence: Tel.: + 2348026002941; E-mail address: oluwafemiaina100@gmail.com; ORCID: https://orcid.org/0000-0002-2988-6496 (Oluwafemi S. Aina)

[1]Drug Discovery Laboratory, Chemistry Department, University of Lagos, Lagos, Nigeria; [2]Biological Sciences Department, Trinity University, Lagos, Nigeria.

Other authors:
Email: mujeeb.rofiu@gmail.com; ORCID: https://orcid.org/0009-0008-1744-4034 (Mujeeb O. Rofiu); Email: owosenikafayat@gmail.com; ORCID: https://orcid.org/0009-0007-4294-1166 (Kafayat A. Owoseni-Fagbenro); Email: ladams@unilag.edu.ng; ORCID: https://orcid.org/0000-0002-0010-5721 (Luqman A. Adams); Email: familonio@unilag.edu.ng; ORCID: https://orcid.org/0000-0002-5480-232X (Oluwole B. Familoni);

Citation on this article: Aina SO, Rofiu MO, Owoseni-Fagbenro KA, Adams LA, Familoni OB. Inhibitors of Plasmodium falciparum dihydrofolate reductase-thymidylate synthase: In-silico evaluation of phenylpiperazinyl derivatives. Investigational Medicinal Chemistry and Pharmacology (2025) 8(2):109; Doi: https://dx.doi.org/10.31183/imcp.2025.00109

Background

Malaria remains a significant global infectious disease characterized by severe fever, presenting an ongoing concern for public health [1]. In 2022, the World Health Organization (WHO) reported an estimated global burden of malaria in 2020, ranging between 200 to 300 million cases, resulting in approximately 627,000 deaths [2]. *Plasmodium falciparum*, the most widespread and formidable species of the parasite particularly affects Africa [3]. In the recent times there have been emergence of drug-resistant strains of *P. falciparum*, creating a distressing situation due to the diminished effectiveness of current medications (Figure 1). These challenges have inspired initiatives to explore new drugs or repurposing of existing chemical compounds as strategies to more enduring medical intervention. An innovative approach to addressing drug resistance in malaria involves investigating alternative biological compounds that can affect different target sites. Drug resistance in malaria parasites, especially resistance to antifolates that target dihydrofolate reductase (DHFR), presents a formidable barrier to malaria control [4].

DHFR is a component of the multifunctional enzyme dihydrofolate reductase-thymidylate synthase (DHFR-TS), which in *P. falciparum* is a confirmed target for antifolate antimalarials. The enzyme DHFR exists as a dimer, and its interactions between domains are significantly influenced by the junction region and plasmodium-specific sequences [5]. Unfortunately, well-known inhibitors such as pyrimethamine and cycloguanil, including their derivatives, have encountered widespread resistance at positions 108 and 16, as well as changes in the overall configuration of the enzyme's main chain [6]. Combinations of inhibitors with sulfa-drugs, which target dihydropteroate synthase (DHPS) in the folate synthesis pathway, are not immune to the threat of resistance.

In-silico studies showed that piperazine derivatives could target Plasmodium plasmepsin II enzyme. Thirteen new phenylpiperazines derivatives activities against *P. falciparum* [7] were investigated. Similarly, phenyl piperazines analogs were investigated for *in-vitro* and toxicity activities against *P. falciparum* Colombian FCR-3 strain and *Leishmania infantum* (Figure 2) [8]. A series of 27 flavonoid derivatives having various substitution patterns on both the piperazinyl and flavone units, were evaluated against *P. falciparum* to observe effects on the compounds' antiplasmodial activity [9]. The most potent compounds demonstrated *in-vitro* micromolar to submicromolar activity levels range against both chloroquine-sensitive and -resistant strains of *P. falciparum*. Specifically, the compounds that exhibited the highest activity featured a 2,3,4-trimethoxybenzylpiperazinyl chain attached to the flavone at the 7-phenol group (Figure 2) [9-10]. Thus, the aim of the study is to investigate the potentials of phenylpiperazinyl derivatives as safe alternative safe and potent antifolate enzyme inhibitor towards obtaining lead candidates in malaria treatment.

Methods

Hypothetical compounds, piperazine-1,4-diylbis(phenylmethanone) A1, its reduced mono- and di- alcohol derivative A2 and A3 respectively (Figure 2) were conceptualized and drawn using ChemDraw 14. The strategy adopted was designed to obtain insights into the binding interactions between compounds A1-A3 and the specific amino acid residues essential for antifolate targets.

Toxicity prediction of hypothetical compounds A1-3

The hypothetical compounds A1-3 underwent toxicity testing by loading their SMILES representation (drawn using ChemDraw 14.0 and saved as an .sdf file) into Protox II web server (https://tox-new.charite.de/protox_II/). The extracted data from the web server provided *in-silico* information on hepatoxicity, carcinogenicity, immunotoxicity, mutagenicity and cytotoxicity [11].

Conversion of selected reference antimalarial active compounds into pdbqt format

Ten antimalarial drugs were selected; artesunate, doxycycline, tafenoquine, amodiaquine, artemether, lumefantrine, primaquine, piperaquine, mefloquine and chloroquine for use in this study. Their structures were obtained from PubChem (https://pubchem.ncbi.nlm.nih.gov/) and docked as ligands for comparative purposes. The structures of these drugs active compounds were downloaded and saved in the .sdf format, and their corresponding SMILES representations were then uploaded onto the Protox II web server (https://pubchem.ncbi.nlm.nih.gov/) for virtual toxicity profiles screening and compliance with drug-likeness rules [12].

Selection of P. falciparum dihydrofolate reductase-thymidylate synthase receptor

The crystal structure of the *P. falciparum* dihydrofolate reductase-thymidylate synthase (DHFR-TS) protein molecule, with a resolution of 2.60 Å, was acquired from the Protein Data Bank at rcsb.org (https://www.rcsb.org/) in the pdb format. Thereafter, it was processed using BIOVIA Discovery Studio DS 2020 to eliminate any unwanted ligands and water molecules. Additionally, polar hydrogen atoms were added to the structure as required.

In-silico drug-likeness and ADME predictions

The compounds A1-3 were investigated for drug-likeness using SwissADME (http://www.swissadme.ch/index.php) to predict crucial adsorption, distribution, metabolis and excretion (ADME) parameters. The SMILES representations of these compounds were uploaded onto the web server. The extracted data were processed to obtain results which were crucial to gain insights on their potential drug-likeness.

Bioactivity scores of Phenylpiperazinyl derivatives A1 – A3

Vital physicochemical parameters and bioactivity score predictions of the hypothetical compounds A1-3 was carried out using molinspiration webserver (http:// https://www.molinspiration.com/). This analysis provides the basis for evaluation of bioactive compounds compliance with Pearson correlation co-efficient towards identifying potential lead drug candidates. The SMILES representations of the compounds were submitted to the web server, and the resulting data were analyzed.

DFT Studies of Phenylpiperazinyl derivatives A1 – A3

The conformational search was performed using Spartan 14 Conformer Distribution with Molecular Mechanics/MMFF, and the most stable conformers were chosen [13]. Geometry optimization

and Frequency calculation of the best conformer for each piperazines were simulated without constraints using the density functional theory (DFT) method with the functional (B3LYP) and 6-31G** (basis set) [14-15]. The optimized structures, the Frontier molecular orbitals, dipole moment and electrostatic potential maps were generated using the software from the TDDFT calculations. Global reactivity descriptors like electronegativity (χ), chemical potential (μ), electrophilicity (ω), global hardness (η) and global softness (S) were derived from the EHOMO and ELUMO, respectively [16].

Molecular docking study

Evaluation of the inhibitory potential of the designed compounds A1 – 3, and the selected reference drugs active chemical compounds were investigated through docking simulations performed using the PyRx 0.8 AutoDock Vina Wizard. The macromolecules were initially converted to Autodock format, and a flexible ligand to rigid protein approach was employed. All possible binding sites on the target protein were explored during the docking process. The docking calculations were performed within a cubic grid of dimensions 90 × 75 × 60 centered on the protein, encompassing the entire protein structure. This process lasted approximately one hour. A grid spacing of 1.00 Å was utilized to generate the grid maps using the autogrid module of AutoDock Tools. Each ligand underwent nine independent runs to ensure accuracy. Based on the identified potential binding sites, energetically favorable binding conformations were selected using AutodockVina [17]. The binding modes, along with their respective binding affinities and RSB (upper and lower) values, were obtained to guide the selection of the highest scoring binding conformation for each ligand. The binding mode with the best binding affinity was chosen. The ligand-protein complexes were analyzed using DS Visualizer. All software applications were executed on PC-based machines running the Microsoft Windows 10 operating system.

Results and Discussion

Toxicity prediction of designed drug-candidate A1-A3

The toxicity profiles (hepatoxicity, carcinogenicity, immunogenicity, mutagenicity, and cytotoxicity) [11] of the test compounds A1, A2 and A3 and ten standard reference drugs; artesunate, doxycycline, tafenoquine, amodiaquine, artemether, lumefantrine, primaquine, piperaquine, mefloquine, and chloroquine obtained upon subjecting these compounds to virtual investigations using Protox II are as outlined in Table 1. Notably, while all the hypothetical compounds A1-A3 exhibited non-toxicity, nine out of the ten reference drugs exhibited one or more violations, with the only exception being Mefloquine (Table 1). Therefore, mefloquine was adopted for further virtual studies alongside the lead compounds.

In-silico drug-likeness and ADME predictions

The results presented in Table 2 and Figure 3 indicate that the designed compounds A1-A3 exhibit characteristics in compliance with the Rule of Five (RO5) with zero violation to drug-likeness rules [12]. They show suitable number of hydrogen bond donors (0-2 for nitrogen-hydrogen and oxygen-hydrogen bonds) and for hydrogen bond acceptors (4-7 for nitrogen or oxygen atoms), which fall within the recommended ranges (<5 and <10, respectively). Their molecular weights were within range aligning with the guideline of 150 to 500 g/mol. Interestingly, all the three designed compounds A1, A2, and A3 exhibit excellent gastrointestinal (GI) absorption rates and are permeable to blood-brain barrier (BBB) intercellular movement, consequently acting as potential drug leads for both gastrointestinal and nervous system needs (Figure 3(d)). These characteristics can be attributed to specific structural features, such as the presence of the oxygen atoms of the carbonyl and the hydroxy groups in addition to the nitrogen atoms of the central piperazinyl moiety. Furthermore, while compound A1 is a non-substrate, A2 and A3 are identified as substrates for P-glycoprotein (P-gp) based on studies conducted by Klopman *et al*. [18]. All three lead compounds A1-A3 demonstrated good oral bioavailability, with a value of 0.55, with no violation according to Lipinski *et al*. [12].

Physicochemistry of designed compounds A1-A3

Figure 3(a-c) revealed the total compliance of the designed compounds A1 - A3 with physicochemical space for oral bioavailability where LIPO (lipophilicity): -0.7 < XLOG3 < +5.0; SIZE: 150 g/mol < MV < 500 g/mol; POLAR (polarity): 20 A^2 < TPSA < 130 A^2; INSOLU (insolubility): -6 < Log S (ESOL) < 0; INSATU (insaturation): 0.25 < Fraction Csp^3 < 1; FLEX (flexibility): 0 < No. of rotatable bonds < 9. BOILED-Egg graphical output (Figure 3(d)) is an intuitive method to predict simultaneously two key ADME parameters, i.e. the passive gastrointestinal absorption (HIA) and brain access (BBB) relying on WLOGP and TPSA physicochemical descriptors for lipophilicity and apparent polarity [19]. The egg-shaped classification plot includes the yolk (physicochemical space for highly probable BBB permeation) and the white albumen (physicochemical space for highly probable HIA absorption). Active efflux from the CNS or to the gastrointestinal lumen (an important active efflux mechanism involved in those biological barriers) by color-coding also revealed blue dots for P-gp substrates (PGP+) and red dots for P-gp non-substrate (PGP−) [20]. Both BBB and HIA compartments are not mutually exclusive, and the outside grey region stands for molecules with properties implying predicted low absorption and limited brain penetration. BOILED-Egg plot has proven straightforward interpretation and efficient translation to molecular design in a variety of drug discovery settings. Figure 3(d) revealed compound A1 (Molecule 1) to be P-gp non-substrate (PGP−) with active influx/efflux from the CNS while compounds A2 and A3 (Molecule 2 and 3) are both P-gp substrates (PGP+) with active CNS efflux/influx mechanism.

Bioactivity score

The potential candidacy of drug leads can be assessed by evaluating their bioactivity scores. In Figure 3(e), it can be observed that all the compounds A1-A3 generally exhibit high or moderate bioactivity across various parameters. Bioactivity scores for organic molecules are interpreted as active (when the bioactivity score > 0), moderately active (when the bioactivity score lies between −5.0 and 0.0), and inactive (when the bioactivity score < −5.0). Specifically, compound A1 displays high activity in one out of the six parameters, with bioactivity scores 0.03 glycoprotein receptors (GPCR) while A2 and A3 only exhibit moderate activities. All the designed compounds demonstrated moderate bioactivity as kinase inhibitors (KI) (with scores ranging from -0.03 to -0.08), which suggests their potential to inhibit cancer cells [20]. They also exhibit moderate bioactivity as protease inhibitor (PI) (with scores of -0.03 to -0.04) suggesting their potential to impede the maturation of new HIV cells [21]. Additionally, as moderate nuclear

receptor ligands (with scores of 0.18 and 0.26, respectively) and ion channel modulators (ICM) (scores ranging between -0.08 and -0.21) indicates their ability to interact with hydrophobic molecules such as fatty acids, cholesterol, and lipophilic hormones [22-23]. The designed compounds A1-A3 possess ability to regulate metabolic enzymes and promoter proteins, among other functions moderately [24] as revealed in their values, also as enzyme inhibitor (with a score of -0.05 to -0.18), indicating its capability to bind to additional sites on the enzyme [10]. Among the hypothetical compounds, A1 exhibited overall best activity especially as GCPR, ICM, KI, PI and EI while A2 exhibits the least bioactivity score especially as ion channel modulators (ICM) and nuclear reactor ligand.

Structural analysis of reactivity of designed compounds through DFT studies

The chemical structure of a candidate drug compound influences its effectiveness. Therefore, the chemical reactivity of the test compounds A1, A2, and A3 were investigated through DFT analysis. The optimized structures and the calculated infrared spectra (IR) of compounds A1, A2 and A3 by DFT method using B3LYP functional and 6-31G** basis set are shown in Figure 4 while the obtained calculated parameters are displayed in Table 3. The results revealed that compound A1 has the highest electron affinity (EA) whereas compound A2 indicated the lowest ionization potential (IP). IP and EA obtained for the test compounds are the negative numerical values of EH and EL respectively (Table 3), hence the high EA of compound A1 suggest its strong affinity to accept electron from other species whereas compound A2 revealed loss of electrons due to its lower IP value [25]. This observation points to the fact that the binding energy trend of the test compounds is a function of EA energy of the molecules [24]. Furthermore, compound A3 relatively has the highest value of the global chemical hardness (η), chemical electrophilicity (ω) and electronic chemical potential (μ) whereas compound A2 displayed the highest chemical softness S value. This shows that compound A3 is less reactive unlike compound A2 which displayed the lowest chemical hardness and highest softness values. Additionally, the high μ value observed for A3 is suggestive of its good electron acceptor potential comparatively. Generally, a reagent with a high electronic chemical potential μ is a good electron acceptor, whereas a reagent with small electronic chemical potential μ is a good electron donor [26]. The μ values of compounds A1, A2 and A3 explains the obtained binding energy trend of the test molecules with (*P. falciparum* dihydrofolate reductase-thymidylate synthase (PDB ID: 3UM8) receptor with compound A1 exhibiting the highest binding energy. The electron acceptor ability of test molecules A1, A2 and A3 were illustrated through conventional hydrogen bonding of these molecules with the target. For instance, in compound A1, one of the carbonyl groups form hydrogen bonding with Ala_{16} of the receptor 3UM8 by accepting electrons from the amino group on the residue (Figure 5(1a-c)). However, compound A3 also shows a non-conventional hydrogen bonding by donating electrons to the carbonyl on Ile_{164} residue (Figure 5(3a-c)). The electrophilicity ω of the studied scaffolds also support this explanation with A1 having the highest ω value of 2.393 eV. The molecular electrostatic potential (MEP) surfaces mapped over the total density of the geometrically optimized molecules A1, A2 and A3 are presented in Figure 4(a-c). The MEP maps revealed the charge distribution around the molecules and describes enhanced electrophilicity or nucleophilicity of the studied molecules [27]. The color map ranging from the region of red to blue depicts increase in nucleophilicity of the surface. The red regions are areas of nucleophilic attack on the molecular surface and blue regions are feasible for electrophilic attack; the green regions show areas of neutral charge. The hydrogen bonding shown by A1 and A3 with the target molecule 3UM8 was due to its electrophilic attack on the receptor at residues Ala_{16} and Ile_{164} respectively. The optimized structures of A1 – A3 and their calculated infrared spectra are also presented in Figure 4(d-f).

Molecular docking study

The findings from the docking simulations of ligands A1, A2 and A3 and reference drugs against *Plasmodium falciparum* dihydrofolate reductase-thymidylate synthase are summarized in Table 4. The binding energies for compound A1 (-9.20 kcal/mol) is comparable with the best reference drug, doxycycline (-9.00 kcal/mol). While the reduced derivative A2 performed below three of the reference drugs (Artesunate, Doxycycline and Tafenoquine), it however performed better than seven other antimalarial drugs. The extracted 3D structures revealing interactions of the best ligand and reference drug with *Plasmodium falciparum* dihydrofolate reductase (PDB ID: 3UM8) are presented in Figure 5(1a-c, 2a-c) revealing the binding of specific amino acid residues responsible for the reduction of DHFR to THFR for protein's translation, normal mutations and growth (e.g. Alanine to Valine), for reproduction (Phenylalanine and Leucine), for resistance, invasion and survival (Ileucine and Asparagine) and reproduction (mutations of Threonine to Serine /Asparagine). Table 5 and Figure 5 (1a-c, 2a-c) confirmed these unique interactions within the A1-3UM8 and Artesunate-3UM8 complexes exhibiting inhibition of some similar amino acid residues (Ala_{16}, Leu_{40} and Ser_{108}). Interactions shown by derivative A2, A3 and the only non-toxic reference drug, Mefloquine are also presented in Figure 5 (3a-c, 4a-c, 5a-c) respectively for comparison.

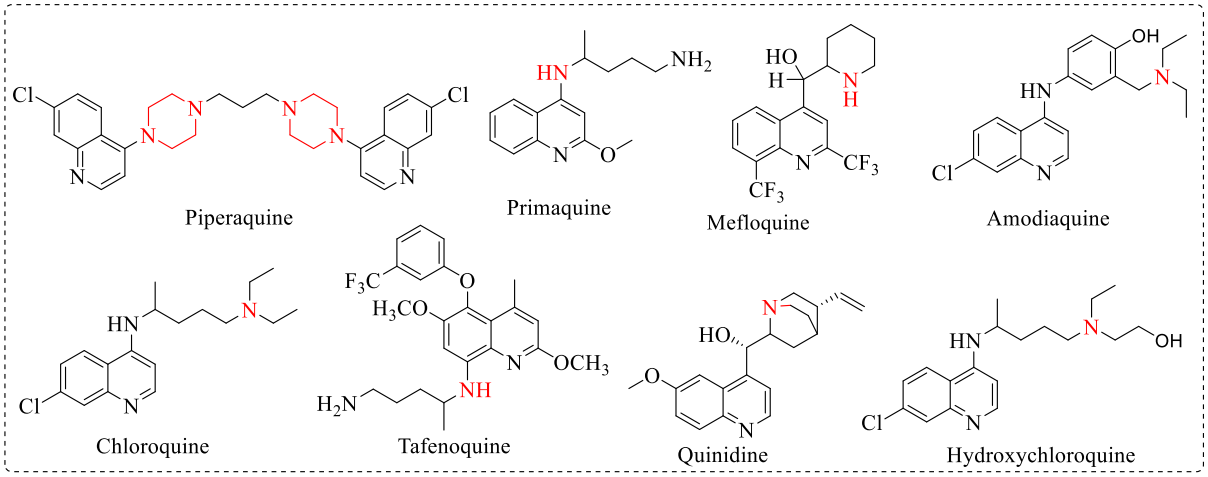

Figure 1. Common antimalarial drugs

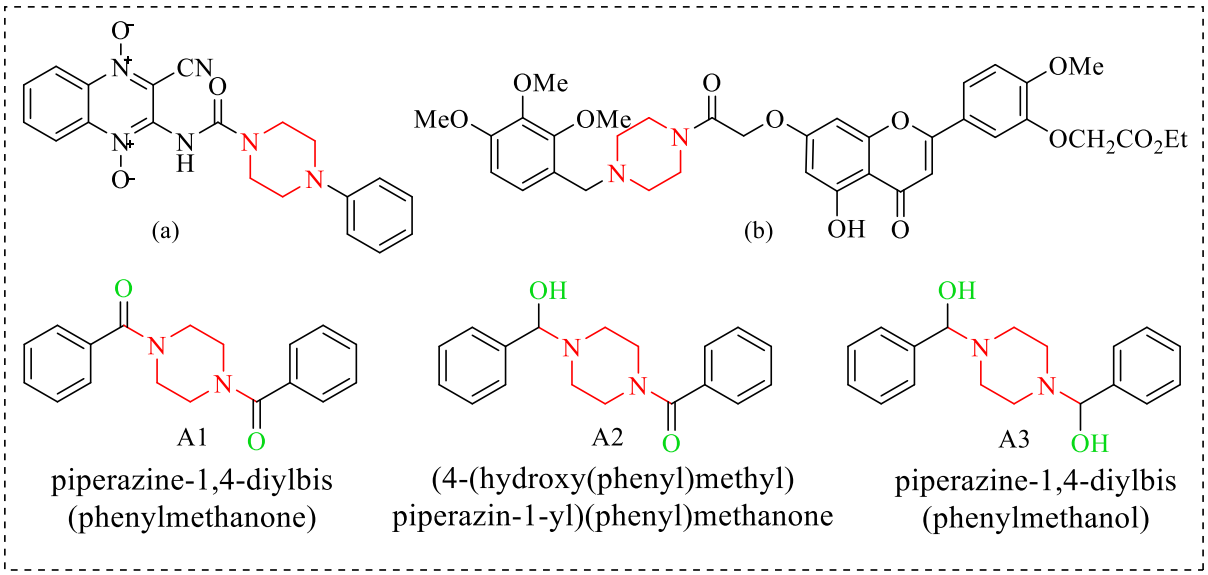

Figure 2. Phenylpiperazine analog (a) investigated for *in-vitro* and toxicity activities against *P. falciparum* Colombian FCR-3 strain and Leishmania infantum; exploration of various substitution patterns on both the piperazinyl and flavone parts flavonoid derivative (b) against *P. falciparum*; and designed phenylpiperazinyl derivatives (A1, A2, A3) as potential antimalarial agents.

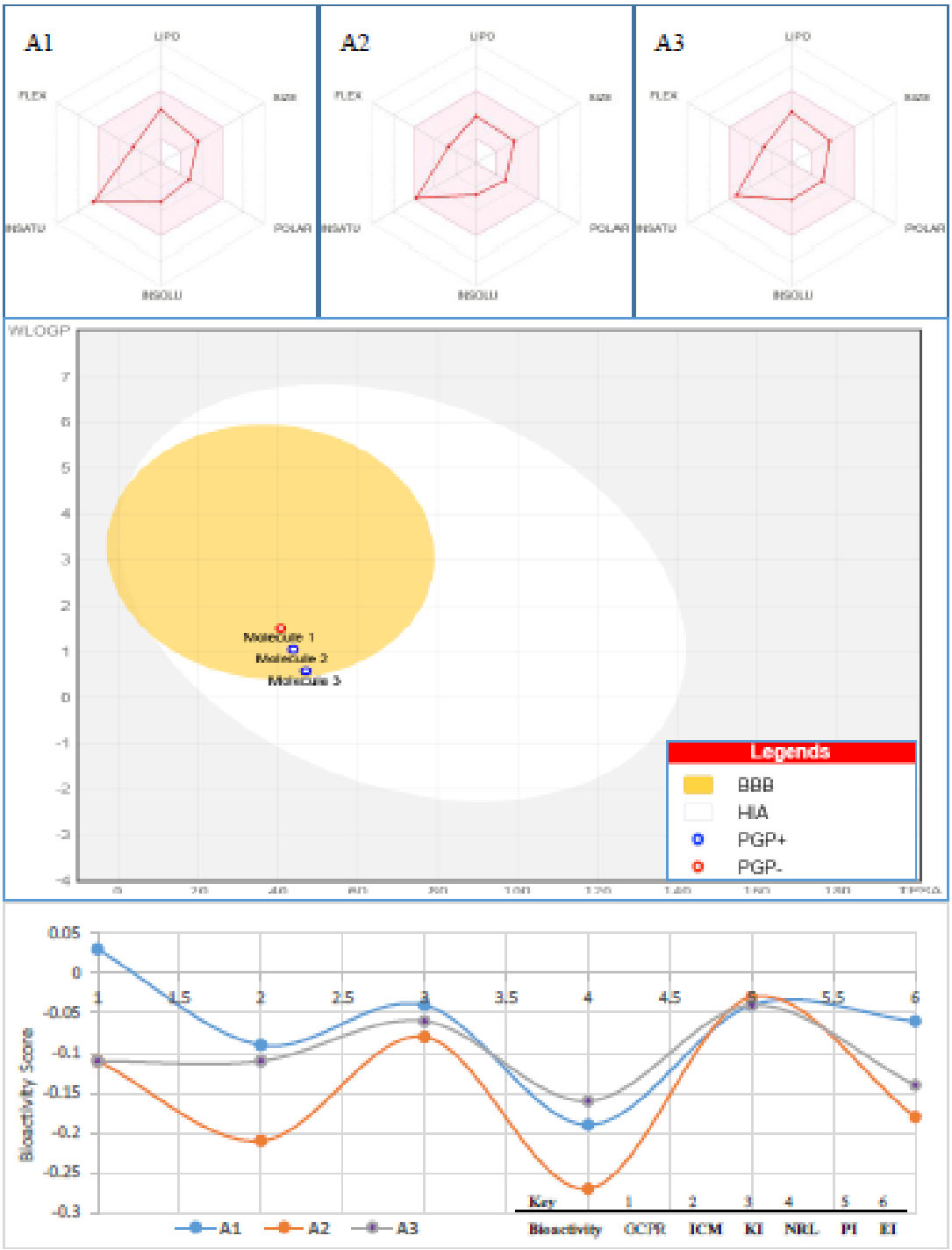

Figure 3. Physicochemical space, BOILED-EGG pharmacokinetics for oral bioavailability and Bioactivity score of phenylpiprazinyl derivatives A1, A2 and A3.

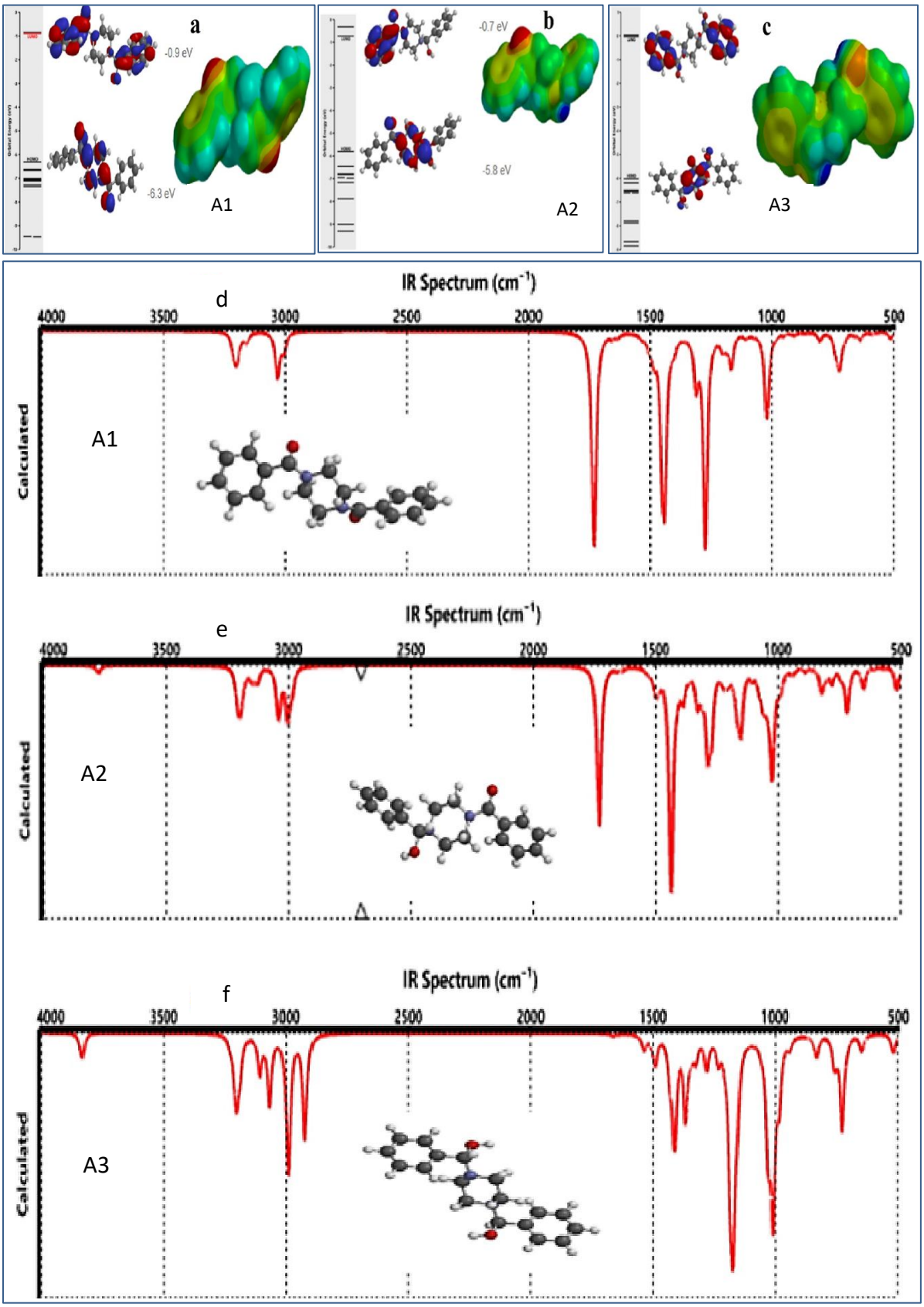

Figure 4. Frontier molecular orbital (HOMO and LUMO) diagram, molecular electrostatic potential map, calculated infrared spectra and optmized structure of compounds A1, A2. A3.

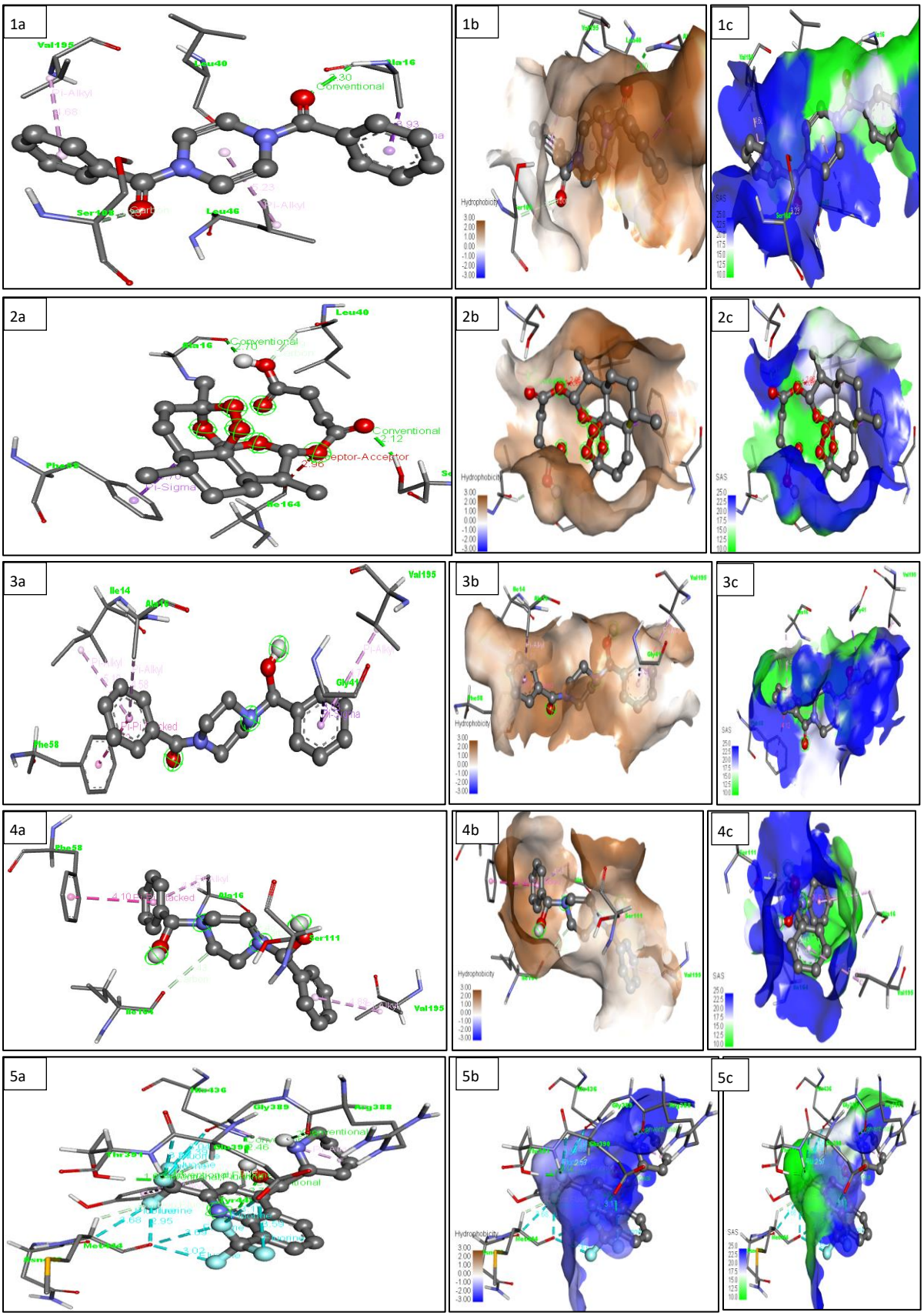

Figure 5. 3D structures of derivative A1-DHFR (1), Artesunate-DHFR (2), A2-DHFR (3), A3-DHFR (4) and Mefloquine-DHFR (5) complexes showing bond length and binding residues (a), hydrophobicity and hydrophilicity (b) and solvent area accessibility surface interaction (c).

Table 1. Toxicity prediction of compounds A1-A3 and standard drugs against *P. falciparum* DHFR-TS (Protox II webserver)

Target	A1	A2	A3	Mefloquine	Piperaquine
Hepatotoxicity	Inactive (0.95)	Inactive (0.93)	Inactive (0.92)	Inactive (0.75)	Inactive (0.78)
Carcinogenicity	Inactive (0.73)	Inactive (0.66)	Inactive (0.67)	Active (0.76)	Inactive (0.71)
Immunotoxicity	Inactive (0.99)	Inactive (0.99)	Inactive (0.99)	Inactive (0.84)	Active (0.93)
Mutagenicity	Inactive (0.78)	Inactive (0.77)	Inactive (0.76)	Inactive (0.68)	Active (0.50)
Cytotoxicity	Inactive (0.84)	Inactive (0.84)	Inactive (0.86)	Inactive (0.74)	Inactive (0.82)
Target	**Amodiaquine**	**Artemeter**	**Lumefantrine**	**Doxycycline**	**Tafenoquine**
Hepatotoxicity	Inactive (0.61)	Inactive (0.77)	Inactive (0.70)	Active (0.54)	Inactive (0.78)
Carcinogenicity	Active (0.61)	Inactive (0.66)	Inactive (0.61)	Inactive (0.77)	Inactive (0.63)
Immunotoxicity	Active (0.99)	Active (0.92)	Active (0.99)	Active (0.99)	Active (0.99)
Mutagenicity	Inactive (0.75)	Inactive (0.60)	Inactive (0.60)	Inactive (0.95)	Active (0.54)
Cytotoxicity	Inactive (0.53)	Inactive (0.94)	Inactive (0.67)	Inactive (0.90)	Inactive (0.63)
Target	**Primaquine**	**Chloroquine**			
Hepatotoxicity	Inactive (0.84)	Inactive (0.90)			
Carcinogenicity	Inactive (0.59)	Inactive (0.66)			
Immunotoxicity	Active (0.99)	Active (0.69)			
Mutagenicity	Active (0.79)	Active (0.94)			
Cytotoxicity	Inactive (0.61)	Inactive (0.93)			

Table 2. Evaluation of drug likeness and oral bioavailability of A1, A2 and A3 in comparison with Mefloquine

Parameters	A1	A2	A3	Mefloquine
Molecular weight	294.35	296.36	298.38	378.31
Hydrogen bond donor (HBD)	0	1	2	2
Hydrogen bond acceptor (HBA)	2	3	4	9
#Rotatable bonds	4	4	4	4
TPSA	40.62	43.78	46.94	45.15
Lipinski #violations	0	0	0	0
Ghose #violations	0	0	0	0
Veber #violations	0	0	0	0
Egan #violations	0	0	0	0
Muegge #violations	0	0	0	0
PAINS #alerts	0	0	0	0
Brenk #alerts	0	0	0	0
Leadlikeness #violations	0	0	0	2
Bioavailability score	0.55	0.55	0.55	0.55

Table 3. DFT Calculated Parameters of A1, A2 and A3

DFT Parameters	A1	A2	A3
ZPE (kJ/mol)	866.09	926.32	984.59
EH	-6.32	-5.81	-6.01
EL	-0.89	-0.73	-0.03
EGap	5.43	5.08	5.98
η	2.715	2.54	2.99
S	0.184	0.196	0.167
μ	3.605	3.27	3.02
IP	6.32	5.81	6.01
EA	0.89	0.73	0.03
χ	-3.605	-3.27	-3.02
ω	2.393	2.104	1.525
$\omega+$	0.93	0.787	0.385
$\omega-$	4.535	4.057	3.409
Dipole Moment (debye)	1.32	2.7	0
Sol Ener. (kJ/mol)	-27.93	-27.24	-21.58
Polarizability	65.35	65.84	66.03
Ovality	1.46	1.47	1.49

Table 4. Binding Energies of Designed Compounds and Reference Antimalarial Drugs

Ligand	B/E	rmsd/ub	rmsd/lb
3um8_A1_E=306.61	-9.2	0	0
3um8_Doxycycline_E=948.86	-9.0	0	0
3um8_Tafenoquine_E=732.40	-8.8	0	0
3um8_A2_E=225.29	-8.8	0	0
3um8_Artemeter_E=650.55	-8.6	0	0
3um8_Amodiaquine_E=471.01	-8.5	0	0
3um8_A3_E=313.29	-8.2	0	0
3um8_Mefloquine_E=499.35	-7.9	0	0
3um8_Piperaquine_E=843.34	-7.6	0	0
3um8_Lumefantherine_E=859.73	-7.3	0	0
3um8_Primaquine_E=279.57	-7.1	0	0
3um8_Chloroquine_E=480.75	-5.6	0	0

Table 5. Comparison of amino acid residues of phenylpiperazinyl A1 and Artesunate

A1-3UM8 complex	Ala 16	Leu 40	Ser 108	Leu 46	Val 195
Artesunate-3UM8 complex	Ala 16	Leu 40	Ser 108	Ile 164	Phe 58

Conclusion

Based on our study, drug resistance to antifolates targeting dihydrofolate reductase (DHFR) in *Plasmodium falciparum* presents a significant challenge. Our *in-silico* evaluation of the compounds piperazine-1,4-diylbis(phenylmethanone) (A1) and its derivatives A2 and A3 demonstrated potentials as antimalarial drug candidates. All three compounds were predicted to be non-toxic, unlike most of the corresponding reference drugs with the notable exception of Mefloquine. Compound A1 showed the best overall bioactivity, with values for GCPR, ICM, KI, PI, and EI ranging from +0.03 to -0.19 with its enzymatic activity comparable to Artesunate. A BOILED Egg Model prediction revealed that A1 is a P-gp non-substrate, indicating active CNS penetration, while A2 and A3 are P-gp substrates with a high probability of brain penetration. The chemical hardness trend was found to be moderate for A1, soft for A2, and hard for A3. The investigated amino acids were all hydrophobic with excellent solvent accessibility, which supports good intercellular water-lipid interactions. Therefore, these compounds, particularly A1, are presented as potential non-toxic alternatives for antimalarial drug development.

Abbreviations

#HA: Number of Hydrogen Bond Acceptors
#HD: Number of Hydrogen Bond Donors
#rot_b: Number of Rotatable Bonds
Å: Ångström (unit of length, 10^-10 meters)
ADME: Absorption, Distribution, Metabolism, and Excretion
B3LYP: Becke, 3-parameter, Lee-Yang-Parr (functional used in DFT calculations)
BBB: Blood-Brain Barrier
BOILED-Egg: Brain or IntestinaL Estimate D Permeation Graph
CNS: Central Nervous System
CYP: Cytochrome P450
DFT: Density Functional Theory
DHFR: Dihydrofolate Reductase
DHPS: Dihydropteroate Synthase
DNA: Deoxyribonucleic Acid
EA: Electron Affinity
EGap: Energy Gap
EH: Energy of HOMO
EHOMO: Energy of the Highest Occupied Molecular Orbital
EL: Energy of LUMO
ELUMO: Energy of the Lowest Unoccupied Molecular Orbital
ESI: Electrospray Ionization
ESOL: Estimation of Aqueous Solubility
GPCR: G-Protein Coupled Receptor
HIA: Human Intestinal Absorption
HOMO: Highest Occupied Molecular Orbital
IP: Ionization Potential
IR: Infrared Spectroscopy
KI: Kinase Inhibitor
LIPO: Lipophilicity
Log S: Logarithm of Solubility
LUMO: Lowest Unoccupied Molecular Orbital
MEP: Molecular Electrostatic Potential
MMFF: Merck Molecular Force Field
MV: Molecular Volume
NMR: Nuclear Magnetic Resonance
PAINS: Pan-Assay Interference Compounds
PI: Protease Inhibitor
P-gp: P-glycoprotein
PDB: Protein Data Bank
P. falciparum: Plasmodium falciparum
Protox II: Toxicity Prediction Webserver
RO5: Rule of Five

RSB: Root-Mean-Square Deviation (upper and lower bounds)
S: Global Softness
SMILES: Simplified Molecular Input Line Entry System
THFR: Tetrahydrofolate Reductase
TPSA: Total Polar Surface Area
TS: Thymidylate Synthase
WHO: World Health Organization
WLOGP: Wildman-Crippen LogP (octanol-water partition coefficient)
XLOGP: Logarithm of the Partition Coefficient (Octanol/Water)
ZPE: Zero-Point Energy
χ: Electronegativity
ω: Electrophilicity
Ω: Electrophilicity Index
ω-: Negative Electrophilicity
ω+: Positive Electrophilicity
μ: Chemical Potential
η: Global Hardness

Authors' Contribution

OSA virtual screening studies; LAA and OBF designed and supervised the studies; and LAA provide instrumentation for experimental studies, MOB carried out the DFT analysis and interpretation. OSA and MOB wrote the first manuscript draft KO-F, LAA and OBF critically reviewed and edited the manuscript.

Acknowledgments

The authors wish to appreciate the Department of Chemistry University of Lagos for supporting this research.

Conflict of interest

The authors declare no conflict of interest

Article history:

Received: 13 July 2025
Received in revised form: 14 August 2025
Accepted: 24 August 2025
Available online: 24 August 2025

References

1. Hastings IM, Donnelly MJ. 2005. The impact of antimalarial drug resistance mutations on parasite fitness, and its implications for the evolution of resistance. *Drug Resist Updat.* 8(1-2):43-50.
2. World Health Organization. 2022. *WHO guidelines for malaria, 3 June 2022* (No. WHO/UCN/GMP/2022.01 Rev. 2). World Health Organization.
3. Jensen AR, Adams Y, Hviid L. 2020. Cerebral Plasmodium falciparum malaria: The role of PfEMP1 in its pathogenesis and immunity, and PfEMP1-based vaccines to prevent it. *Immunol Rev.* 293(1):230-52.
4. Vanichtanankul J, Taweechai S, Yuvaniyama J, Vilaivan T, Chitnumsub P, Kamchonwongpaisan S, Yuthavong Y. 2011. Trypanosomal dihydrofolate reductase reveals natural antifolate resistance. *ACS Chem Biol.* 6(9):905-11.
5. A-Elbasit IE, Alifrangis M, Khalil IF, Bygbjerg IC, Masuadi EM, Elbashir MI, Giha HA. 2007. The implication of dihydrofolate reductase and dihydropteroate synthetase gene mutations in modification of Plasmodium falciparum characteristics. *Malaria Journal.* 6:1-8.
6. Yuthavong Y, Yuvaniyama J, Chitnumsub P, Vanichtanankul J, Chusacultanachai S, Tarnchompoo B, Kamchonwongpaisan S. 2005. Malarial (Plasmodium falciparum) dihydrofolate reductase-thymidylate synthase: structural basis for antifolate resistance and development of effective inhibitors. *Parasitology.* 130(3):249-59.
7. Barea C, Pabón A, Galiano S, Pérez-Silanes S, Gonzalez G, Deyssard C, Aldana I. 2012. Antiplasmodial and leishmanicidal activities of 2-cyano-3-(4-phenylpiperazine-1-carboxamido) quinoxaline 1, 4-dioxide derivatives. *Molecules.* 17(8):9451-61.
8. Mendoza A, Pérez-Silanes S, Quiliano M, Pabón A, Galiano S, González G, Garavito G, Zimic M, Vaisberg A, Aldana I. 2011. Aryl piperazine and pyrrolidine as antimalarial agents. Synthesis and investigation of structure-activity relationships. *Exp Parasitol.* 128:97–103.
9. Auffret G, Labaied M, Frappier F, Rasoanaivo P, Grellier P, Lewin G. 2007. Synthesis and antimalarial evaluation of a series of piperazinyl flavones. *Bioorg Med Chem Lett.* 17(4):959-63.
10. Cunico W, Gomes CR, Facchinetti V, Moreth M, Penido C, Henriques MG, Varotti FP, Krettli LG, Krettli AU, da Silva FS. 2009. Synthesis, antimalarial evaluation and molecular modeling studies of hydroxyethylpiperazines, potential aspartyl protease inhibitors, part 2. *Eur J Med Chem.* 44:3816-20.
11. Banerjee P, Eckert AO, Schrey AK, Preissner R. 2018. ProTox-II: a webserver for the prediction of toxicity of chemicals. *Nucleic Acids Res.* 46(1):257-63.
12. Lipinski CA, Lombardo F, Dominy BW, Feeney PJ. 2012. Experimental and computational approaches to estimate solubility and permeability in drug discovery and development settings. *Adv Drug Deliv Rev.* 64:4-17.
13. Willoughby P, Reisbick S. 2019. Generation of Gaussian 09 input files for the computation of 1H and 13C NMR chemical shifts of structures from a Spartan'14 conformational search.
14. Bouzzine SM, Bouzakraoui S, Bouachrine M, Hamidi M. 2005. Density functional theory (B3LYP/6-31G) study of oligothiophenes in their aromatic and polaronic states. *J Mol Struct THEOCHEM. 726(1-3):271-6.**
15. Sıdır İ, Sıdır YG, Kumalar M, Taşal E. 2010. Ab initio Hartree–Fock and density functional theory investigations on the conformational stability, molecular structure and vibrational spectra of 7-acetoxy-6-(2, 3-dibromopropyl)-4, 8-dimethylcoumarin molecule. *J Mol Struct.* 964(1-3):134-51.
16. Muthu S, Renuga S. 2014. Molecular orbital studies (hardness, chemical potential, electronegativity and electrophilicity), vibrational spectroscopic investigation and normal coordinate analysis of 5-{1-hydroxy-2-[(propan-2-yl) amino] ethyl} benzene-^{1}1, 3-diol. *Spectrochim Acta A Mol Biomol Spectrosc.* 118:683-94.
17. Trott O, Olson AJ. 2010. AutoDock Vina: improving the speed and accuracy of docking with a new scoring function, efficient optimization, and multithreading. *J Comput Chem.* 31(2):455-61.
18. Klopman G, Stefan LR, Saiakhov RD. 2002. ADME evaluation: 2. A computer model for the prediction of intestinal absorption in humans. *Eur J Pharm Sci.* 17(4-5):253-63.
19. Montanari F, Ecker GF. 2015. Prediction of drug-ABC-transporter interaction–Recent advances and future challenges. *Adv Drug Deliv Rev.* 86:17–26.
20. Kakinuma T, Hwang ST. 2006. Chemokines, chemokine receptors, and cancer metastasis. *J Leukoc Biol.* 79(4):639-51.
21. Leung D, Abbenante G, Fairlie DP. 2000. Protease inhibitors: current status and future prospects. *J Med Chem.* 43(3):305-41.
22. Barker BS, Young GT, Soubrane CH, Stephens GJ, Stevens EB, Patel MK. 2017. Ion channels. *Conn's Transl Neurosci.* 1:1-4. Academic Press.
23. McEwan IJ. 2009. Nuclear receptors: one big family. *The Nuclear Receptor Superfamily: Methods and Protocols.* 3-18.
24. Schwab A, Fabian A, Hanley PJ, Stock C. 2012. Role of ion channels and transporters in cell migration. *Physiol Rev.* 92(2):1075-1215.
25. Isegawa M, Neese F, Pantazis DA. 2016. Ionization energies and aqueous redox potentials of organic molecules: comparison of DFT, correlated ab initio theory and pair natural orbital approaches. *J Chem Theory Comput.* 12(5):2272-84.
26. Domingo LR, Ríos-Gutiérrez M, Pérez P. 2016. Applications of the conceptual density functional theory indices to organic chemistry reactivity. *Molecules.* 21(6):74.
27. Mumit MA, Pal TK, Alam MAA, Islam MAAA, Paul S, Sheikh MC. 2020. DFT studies on vibrational and electronic spectra, HOMO–LUMO, MEP, HOMA, NBO and molecular docking analysis of benzyl-3-N-(2, 4, 5-trimethoxyphenylmethylene) hydrazinecarbodithioate. *J Mol Struct.* 1220:128715.